ComEX

LETTER

Measuring antenna radiation efficiency in a reverberation chamber and effect of unstirred waves

Katsushige Harima [iD][1, a)] **and Kaoru Gotoh**[1]

Abstract The antenna radiation efficiency of a K-band horn was determined using a reference waveguide method with S-parameters in a reverberation chamber. Numerical analysis was performed to validate the applicability of the measurement method and the measured results. In addition, the effect of unstirred waves on the radiation efficiency measurements was evaluated using the complex S-parameter method for identifying unstirred waves.

Keywords: radiation efficiency, reference waveguide method, reverberation chamber, S-parameter, substitution method, unstirred wave

Classification: Electromagnetic compatibility (EMC)

1. Introduction

Reverberation chambers (RVCs), which create a random electromagnetic environment, are used for electromagnetic compatibility (EMC) measurements [1] such as radiated emissions, radiated immunity, radiation efficiency, and shielding effectiveness, as well as for over-the-air (OTA) evaluations of wireless devices. The standard method for measuring antenna radiation efficiency using an RVC is based on the substitution method [1, 2], where the received power of the antenna under test is compared with that of a reference antenna. However, the reference antenna requires a known radiation efficiency, which is generally not easy to measure. Substitution methods using an antenna a calculable [3] or measurable [4] radiation efficiency and methods that do not require a reference antenna, such as the extended Wheeler cap method [5] and the three-antenna method [6], have been proposed. Of these, the reference waveguide method [4] uses a waveguide with measurable radiation efficiency, although it assumes that the radiation efficiency is equal to the insertion loss. In general, when measuring in an RVC, the transmitting and receiving antennas are placed to avoid direct illumination. This is because unstirred waves are a significant source of measurement uncertainty.

In this paper, we describe the measurement of radiation efficiency using the reference waveguide method with complex S-parameters in an RVC. The assumption regarding antenna insertion loss and radiation efficiency in the reference

[1] Electromagnetic Compatibility Laboratory, National Institute of Information and Communications Technology, Koganei-shi, Tokyo 184-8795, Japan
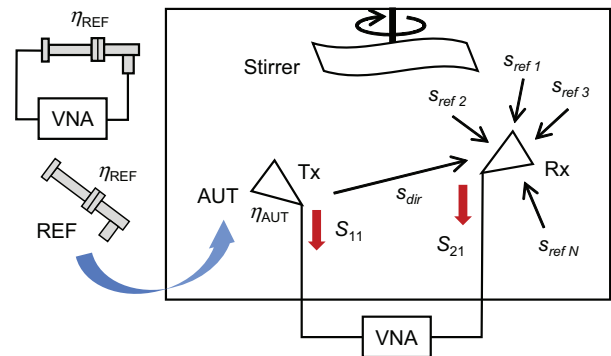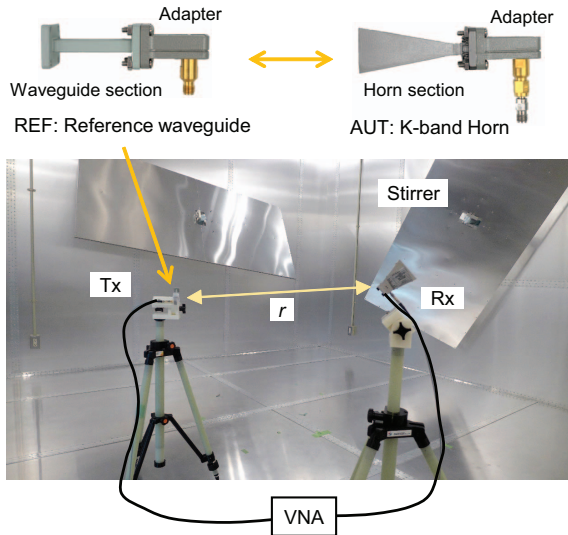
a) harima@nict.go.jp

Fig. 1: Reference waveguide method with S-parameters for determining radiation efficiency in RVC.

waveguide method was validated by numerical simulations. Then, the radiation efficiency of the K-band horn was determined and compared with the calculated values. In addition, the S-parameter method [7] was used to identify the unstirred waves in the chamber and to evaluate the appropriateness of the antenna placement and the effect of the unstirred waves on the radiation efficiency measurements.

2. Reference waveguide method

The transmitting and receiving antennas are placed to avoid direct illumination in an RVC and connected to the network analyzer (VNA), as shown in Fig. 1. The antenna under test (AUT) is used as the transmitting antenna and is replaced by the reference antenna (REF). The radiation efficiency of AUT, η_{AUT}, is expressed using the S-parameters between the transmitting and receiving antennas and the radiation efficiency of REF, η_{REF}, as

$$\eta_{\text{AUT}} = \frac{1 - |\langle S_{11\text{REF}}\rangle_N|^2}{1 - |\langle S_{11\text{AUT}}\rangle_N|^2} \cdot \frac{\langle |S_{21\text{AUT}}|^2\rangle_N}{\langle |S_{21\text{REF}}|^2\rangle_N} \cdot \eta_{\text{REF}}, \quad (1)$$

where $\langle\ \rangle_N$ denotes the average of N samples over one rotation of the stirrer. For AUT and REF, respectively, $S_{21\text{AUT}}$ and $S_{21\text{REF}}$ are the S_{21} parameters, $S_{11\text{AUT}}$ and $S_{11\text{REF}}$ are the S_{11} parameters of the antenna mismatch. The substitution method requires a REF with a known radiation efficiency. In the reference waveguide method [4], a waveguide with a coax-to-waveguide adapter is used as the REF, and the insertion loss of the waveguide is treated as the radiation efficiency η_{REF}.

The S_{21} parameter is expressed as the sum of the direct

Copyright © 2023 The Institute of Electronics, Information and Communication Engineers

Fig. 2: Experimental setup for reference waveguide method.

or unstirred wave component S_{dir} and the reflected wave component S_{ref}, and then the mean value is given by

$$\langle S_{21}\rangle_N = \frac{N \cdot S_{dir}}{N} + \langle S_{ref}\rangle_N. \qquad (2)$$

In an ideal RVC, the complex mean of S_{21} is equal to the direct wave component as the reflected wave component with normal distribution converges to zero [7].

$$\langle S_{21}\rangle_N = S_{dir} \qquad (3)$$

Therefore, the identification of unstirred waves by measuring the S_{21} parameter allows us to confirm the appropriateness of the antenna placement and also to correct its effects using the following [8]:

$$\eta_{AUT} = \frac{1 - |\langle S_{11REF}\rangle_N|^2}{1 - |\langle S_{11AUT}\rangle_N|^2} \cdot \frac{\langle |S_{21AUT} - \langle S_{21AUT}\rangle_N|^2\rangle_N}{\langle |S_{21REF} - \langle S_{21REF}\rangle_N|^2\rangle_N} \cdot \eta_{REF}. \qquad (4)$$

3. Experiments and results

The RVC we used consisted of a shielded enclosure (4.5 m × 4 m × 3 m) and four stirrers (1 m × 2.2 m) mounted on three walls and the ceiling. The transmitting and receiving antennas were arranged at a distance of 1.5 m (= r) to avoid direct illumination and connected to the VNA, as shown in Fig. 2. A K-band (18 GHz to 26.5 GHz) horn antenna as AUT, a WR-42 reference waveguide as REF, and a double-ridged guide horn as the receiving antenna were used. The S_{21} parameters between the antennas and the S_{11} parameters for antenna mismatch were measured while the stirrers were continuously rotated at different speeds. Then the radiation efficiency of the horn antenna was determined using Eq. (1). The rotation period of the stirrers, i.e., the return of the four stirrers to their initial position, was set to 120 s.

3.1 Radiation efficiency of reference waveguid

The reference waveguide method assumes that the insertion loss and radiation efficiency of the waveguide are equivalent. Numerical simulations have been performed to verify
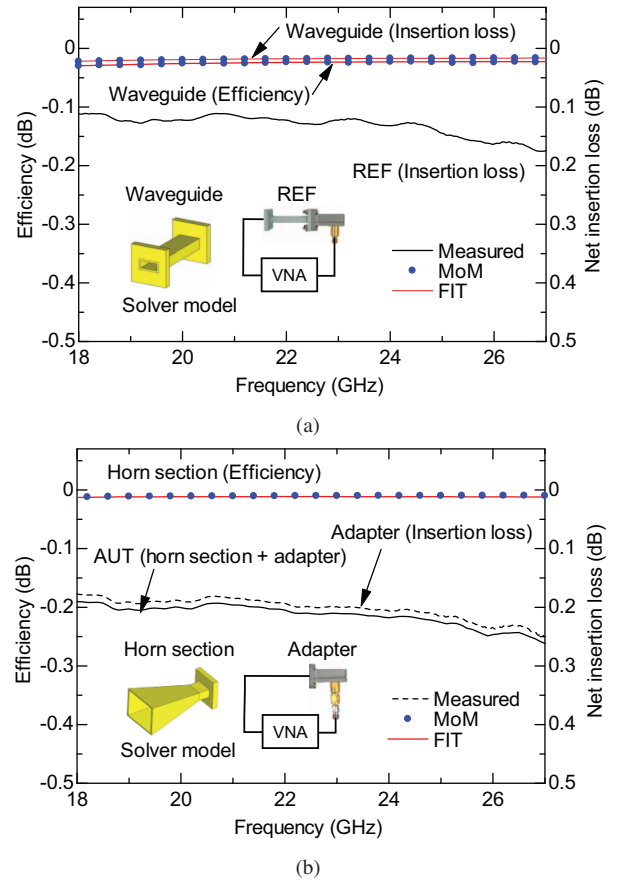

(a)

(b)

Fig. 3: (a) Measured net insertion loss of reference waveguide (REF) and net insertion loss and radiation efficiency of waveguide section simulated by FIT and MoM, respectively. (b) Radiation efficiency of horn antenna (AUT) estimated from measured insertion loss of coax-to-waveguide adapter and radiation efficiency of horn section simulated by FIT and MoM.

that insertion loss can be treated as radiation efficiency. The reference waveguide we used consisted of a 5 cm waveguide section with a flange and a coax-to-waveguide adapter. The net insertion loss and radiation efficiency of the waveguide section were calculated using two electromagnetic field analysis solvers: CST Suite based on the finite integral method (FIT) [9] and WIPL-D based on the method of moments (MoM) [10]. As shown in Fig. 3(a), the simulated results from these solvers are in agreement, and the radiation efficiency is approximately equal to the net insertion loss, although there is a slight loss of 0.007 dB mainly due to the flange at the waveguide port. Thus, the net insertion loss of the reference waveguide can be treated as the radiation efficiency. The insertion loss IL_{net} of the reference waveguide with different port types, coaxial and waveguide, connected directly to the VNA, was measured using the unknown-through calibration method, as shown in the same figure.

$$\eta_{REF} \simeq -IL_{net} = \frac{|S_{21}|^2}{1 - |S_{11}|^2} \qquad (5)$$

Similarly, the radiation efficiency of a K-band horn antenna used as the AUT was estimated for comparison with the measured results. The horn consists of a horn section and
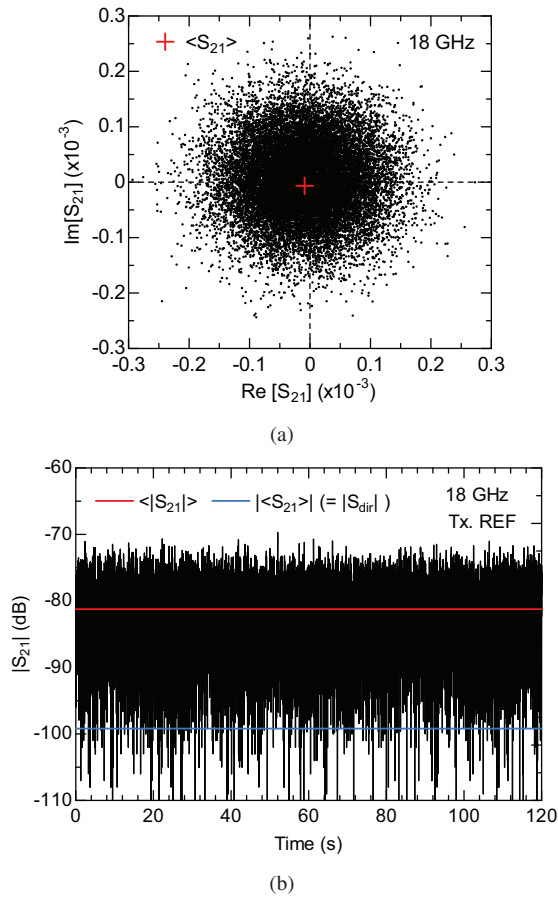
(a)

(b)

Fig. 4: Measured (a) complex values and (b) amplitudes of S_{21} parameters at 18 GHz during one rotation of stirrer: without direct illumination.

Fig. 5: Measured S_{11} parameters of reference waveguide and horn antenna in reverberation and anechoic chambers.

Fig. 6: Determined radiation efficiency of horn antenna: without direct illumination.

a coaxial waveguide adapter. The radiation efficiency of the horn section was calculated using the FIT and MoM solvers, and the insertion loss of the coax-to-waveguide adapter was measured using the VNA. The simulated results from the two different solvers are in agreement, and the radiation efficiency of the horn antenna estimated from the calculated radiation efficiency of the horn section and the measured insertion loss of the adapter section, as shown in Fig. 3(b).

3.2 S-Parameter measurements

The spatial E-field uniformity is improved by increasing the number of positions of the stirrer during one rotation, i.e., the number of samples of the VNA, by time sweep at a fixed frequency (called CW time sweep mode). Because of performance limitations of the VNA used, instead of the CW mode, the VNA was swept at ±10 Hz for each frequency from 18 GHz to 27 GHz to ensure a sufficient number of samples. The mean square value $\langle |S_{21}|^2 \rangle_N$ of the S_{21} term in Eq. (1) was measured by sampling 20,000 points during one rotation of the stirrer for each frequency. The measured complex values and amplitudes of the S_{21} parameters are shown in Fig. 4. The amplitude and phase varied significantly with the rotation of the stirrer, and the complex mean value of the S_{21} parameter ($\langle S_{21} \rangle$), which expresses the unstirred wave component S_{dir}, converged approximately to the origin and its magnitude was very small, 20 dB below the average received level ($\langle |S_{21}| \rangle$), as shown in Figs. 4 (a) and (b). These
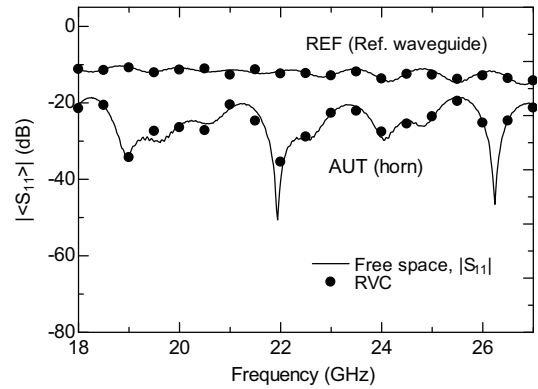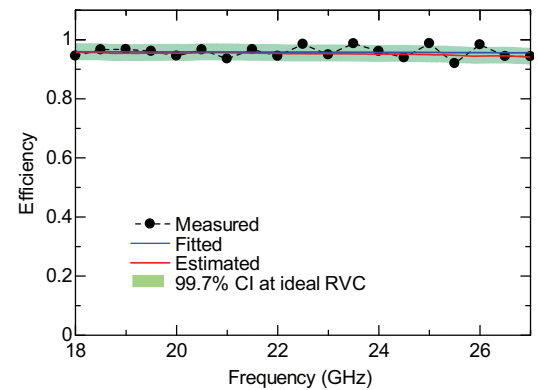
results indicate that the antenna placement is appropriate, i.e., the measured values do not contain any direct or other unstirred waves.

Next, the S_{11} parameters were measured for the antenna mismatch term in Eq. (1). Since the mean of the S_{11} parameter converges faster than that of the S_{21} parameter, the frequency was swept 900 times from 18 GHz to 27 GHz during one rotation of the stirrer, and then the complex mean of the S_{11} parameter ($|\langle S_{11} \rangle|$) was measured. As shown in Fig. 5, the measured $|\langle S_{11} \rangle|$ for the horn antenna and the reference waveguide agree with the free-space measurements of $|S_{11}|$ in the anechoic chamber.

3.3 Determination of antenna efficiency

The radiation efficiency of the horn antenna was determined using Eq. (1) from the S_{21} parameter between the transmitting and the receiving antennas, the antenna mismatches (S_{11}) of the horn antenna and the reference waveguide, and the insertion loss of the reference waveguide, as shown in Fig. 6. Although the fitted straight line of the measured radiation efficiency is in close agreement with the estimate shown in Fig. 3(b), the variation obtained with 20,000 samples is worse than that assumed for an ideal RVC, where the uniformity of the distribution of the mean square of $|S_{21}|$ is expected to be ±0.09 dB with a 99.7% confidence interval (CI) based on interval estimation [11]. This is because the actual uniformity depends on the size of the chamber.
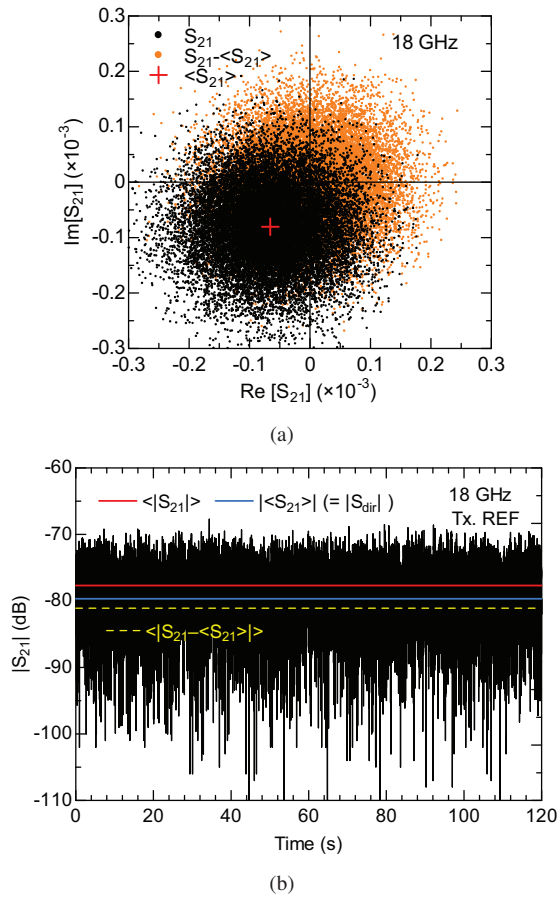
Additionally, the antennas were oriented so that they were

(a)

(b)

Fig. 7: Measured (a) complex values and (b) amplitudes of S_{21} parameters at 18 GHz during one rotation of stirrer: with direct illumination.
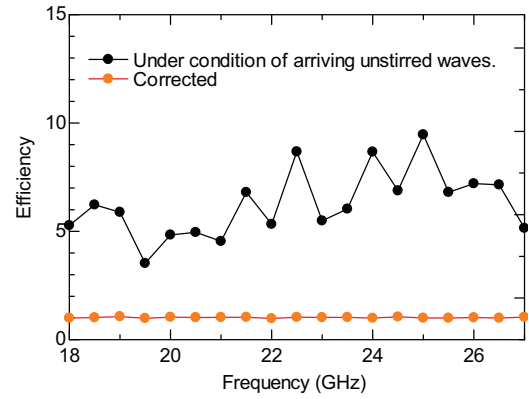

Fig. 8: Determined and corrected radiation efficiency of horn antenna: with direct illumination.

uide method with S-parameters in a reverberation chamber were studied. The assumption in the measurement method that the insertion loss and radiation efficiency of the waveguide are equivalent was verified by numerical analysis using FIT and MoM. The experimental results show that the use of complex S-parameters allows the identification of the unstirred wave component in the received value, confirms the appropriateness of the antenna placement, and reduces the effect of unstirred waves on the radiation efficiency measurement.

directly illuminated at the same separation (r) to evaluate the effect of unstirred waves on the radiation efficiency measurements. The measured complex S_{21} parameter is shown in Fig. 7(a), where the coordinates of the complex mean value of the S_{21} parameter ($\langle S_{21} \rangle$) are shifted from the origin by an amount corresponding to the amplitude of the direct wave. As shown in Fig. 7(b), the received S_{21} values contain a very large direct wave component ($\langle S_{21} \rangle$), and the average received level ($\langle |S_{21}| \rangle$) is 3.5 dB higher than that obtained without the unstirred wave shown in Fig. 4(b), which is the amount corresponding to the direct wave component. To remove the direct wave component, the measurements were corrected using ($S_{21} - \langle S_{21} \rangle$) so that the coordinate of the mean value of S_{21} parameter is at the origin, and then the average corrected value agreed well with the received level of that case without the unstirred wave shown in Fig. 4(b).

Figure 8 shows the measurement results of the radiation efficiency under the condition of direct wave arrival. When the direct wave component is included in the S_{21} measurement, it affects the radiation efficiency obtained. This effect can be reduced by a correction using the complex mean of the S_{21} parameter, even if the received values contain a very large direct wave component.

4. Conclusion

Radiation efficiency measurements using a reference waveg-

References

[1] IEC 61000-4-21, Electromagnetic compatibility (EMC) – Part 4-21: Testing and measurement techniques – Reverberation chamber test methods, 2011.

[2] D. A. Hill, "Reverberation chambers," in *Electromagnetic Fields in Cavities: Deterministic and Statistical Theories*, pp. 91–150, IEEE, 2009. DOI: 10.1002/9780470495056.ch7

[3] D. Senic, D. F. Williams, K. A. Remley, C. -M. Wang, C. L. Holloway, Z. Yang, and K. F. Warnick, "Improved antenna efficiency measurement uncertainty in a reverberation chamber at millimeter-wave frequencies," *IEEE Trans. Antennas Propag.*, vol. 65, no. 8, pp. 4209–4219, Aug. 2017. DOI: 10.1109/TAP.2017.2708084

[4] K. Harima and K. Gotoh, "Determination of antenna radiation efficiency using the reference waveguide to coax adapter method in a reverberation chamber," *IEICE Commun. Express*, vol. 11, no. 11, pp. 715–720, Nov. 2022. DOI: 10.1587/comex.2022XBL0119

[5] C. S. Lee, A. Duffy, and C. Lee, "Antenna efficiency measurements in a reverberation chamber without the need for a reference antenna," *IEEE Antennas Wirel. Propag. Lett.*, vol. 7, pp. 448–450, 2008. DOI: 10.1109/LAWP.2008.2002262

[6] C. L. Holloway, H. A. Shah, R. J. Pirkl, W. F. Young, D. A. Hill, and J. Ladbury, "Reverberation chamber techniques for determining the radiation and total efficiency of antennas," *IEEE Trans. Antennas Propag.*, vol. 60, no. 4, pp. 1758–1770, Apr. 2012. DOI: 10.1109/TAP.2012.2186263

[7] K. Harima, "Determination of EMI antenna factor using reverberation chamber," Proc. 2005 Int. Symp. Electromagn. Compat., Chicago, IL, USA, pp. 93–96, Aug. 2005. DOI: 10.1109/ISEMC.2005.1513480

[8] C. L. Holloway, D. A. Hill, J. M. Ladbury, P. F. Wilson, G. Koepke, and J. Coder, "On the use of reverberation chambers to simulate a Rician radio environment for the testing of wireless devices," *IEEE Trans. Antennas Propag.*, vol. 54, no. 11, pp. 3167–3177, Nov. 2006. DOI: 10.1109/TAP.2006.883987

[9] CST Studio Suite, [online] Available: https://www.3ds.com/

[10] WIPL-D pro CAD, [online] Available: https://wipl-d.com/

[11] J. G. Kostas and B. Boverie, "Statistical model for a mode-stirred chamber," *IEEE Trans. Electromagn. Compat.*, vol. 33, no. 4, pp. 366–370, Nov. 1991. DOI: 10.1109/15.99120